Impact of ultrathin Al_2O_3 diffusion barriers on defects in high-*k* $LaLuO_3$ on Si

S. Shen,[1,a)] Y. Liu,[2] R. G. Gordon,[2] and L. J. Brillson[1]
[1]*Department of Electrical and Computer Engineering, Ohio State University, Columbus, Ohio 43210, USA*
[2]*Department of Chemistry and Chemical Biology, Harvard University, Cambridge, Massachusetts 02138, USA*

(Received 7 January 2011; accepted 6 April 2011; published online 27 April 2011)

We used depth-resolved cathodoluminescence spectroscopy (DRCLS) to measure trap energies and relative densities in metal/high-κ dielectric $LaLuO_3/Si$ stacks, defects produced by $LaLuO_3-Si$ interdiffusion, and suppression of these defects by monolayer-thick Al_2O_3 interlayers. DRCLS reveals deep levels at 3.8, 4.2, and 4.7 eV above the valence band, consistent with $LaLuO_3$ oxygen vacancies predicted by theory and a 5.5 eV band gap. Oxygen annealing produces $LaLuO_3/Si$ interdiffusion that increases 3.8 eV defect density and which a 0.4 nm Al_2O_3 completely removes. Transmission electron microscopy and current leakage results shows that Al_2O_3 prevent $LaLuO_3/Si$ silicate layer formation and dramatically lower defects with oxygen annealing. © *2011 American Institute of Physics*. [doi:10.1063/1.3583462]

As Si-based metal-oxide-semiconductor field effect transistors (MOSFETs) scale down to sub-nanometer dimensions, high leakage current, power consumption, and dielectric breakdown increase as device challenges. High dielectric permittivity (high-κ) insulators represent promising alternatives to SiO_2 in avoiding these effects. Among these, lanthanum lutetium oxide ($LaLuO_3$) possesses many attractive properties for MOSFETs: wide optical band gap (5.6 eV),[1] high and symmetric conduction, and valence band offsets (2.1 eV),[2] dielectric κ above 27, and high crystalline temperature (up to 1000 °C).[3] However, trap densities within high-*k* oxides and at their Si interfaces are substantially higher than for SiO_2 on Si, causing charge trapping, Fermi level pinning, degradation of Si carrier mobility and transient threshold voltage shifts that degrade MOSFET performance.[4] To minimize such trap states and their effect on electronic properties for a specific oxide, one can use depth-resolved cathodoluminescence spectroscopy (DRCLS) (Ref. 5) to monitor trap energies and densities versus substrate preparation,[6,7] deposition or growth method,[8] stoichiometry, interfacial structure, and subsequent processing.[9] Similarly, correlation of observed subband transitions with energy levels of theoretically predicted native point defects can guide growth and processing to suppress specific trap states. Thus Xiong *et al.*[10] have already calculated energy levels for O vacancies in $LaLuO_3$, but observations only now confirm their predictions. Furthermore, chemical reaction, diffusion, and/or altered phases at high-*k* dielectric-semiconductor interfaces can produce new localized states that interlayers must minimize without degrading the insulator's effective oxide thickness (EOT). Here we used DRCLS to measure trap energies and relative densities in metal/high-κ dielectric $LaLuO_3/Si$ stacks, the new defects produced by $LaLuO_3-Si(100)$ interdiffusion, and suppression of these defects by monolayer-thick Al_2O_3 interlayers. DRCLS can generate near-band-to-band and band-to-defect transitions at surfaces, interfaces, and the bulk by varying the electron beam energies, providing unique nanoscale-resolved information about defect distributions.[5,11] We found three major $LaLuO_3$ defects above mid-gap, one of which increases dramatically with oxygen annealing, and two minor defects close to mid-gap. Furthermore, a single monolayer of Al_2O_3 between $LaLuO_3$ and Si substrate acts as a barrier layer that prevents this defect increase and indeed reduces the mid-gap defect states with oxygen annealing. This work confirms the central role of the ultrathin Al_2O_3 barrier layer in removing traps in metal/$LaLuO_3$/Si stacks with oxygen annealing without significantly degrading dielectric EOT.

The $LaLuO_3$ oxide films were deposited in a flow-type atomic layer deposition (ALD) reactor with water vapor alternating with vapors of metal amidinate precursors, to achieve repeated cyclic growth of La_2O_3 and Lu_2O_3. The deposition temperature was 300 °C for $LaLuO_3$. We examined dielectric stacks with two substrate surface terminations: (1) HF-last Si and (2) HF-last Si with ~0.4 nm Al_2O_3 deposited at 300 °C in the same reactor chamber. Following oxide deposition, some of the samples were subjected to oxygen treatments by trapping 1 torr of oxygen gas in the reactor chamber for 10 min at 300 °C. All oxides were amorphous. Finally, all were capped with 10 nm tungsten nitride WN top metal electrodes[12,13] at 385 °C by ALD in the same reactor. Figure 1(a) shows the five different metal/$LaLuO_3$/Si stacks examined by DRCLS: (i) WN/Si; (ii) WN/as-deposited $LaLuO_3$ (20 nm)/Si, (iii) WN/oxygen-treated $LaLuO_3$ (20 nm)/Si, (iv) WN/as-deposited $LaLuO_3$ (20 nm)/Al_2O_3 (0.4 nm)/Si, and (v) WN/oxygen-treated $LaLuO_3$ (20 nm)/Al_2O_3 (0.4 nm)/Si. We examined morphological and electronic properties of these structures by cross-sectional transmission electron microscopy (XTEM) and I-V measurements, respectively.

DRCLS measurements were performed in an ultrahigh vacuum chamber at 80 K with beam voltage E_B varied from 1 to 5 kV in steps of 0.5 kV. Monte Carlo simulations[14] shown in Fig. 1(b) illustrate the rate of electron-hole pair creation generated by the electron cascade and the energy range over which emissions from the $LaLuO_3$ buried layer are maximized. Thus $E_B=1$ keV excitation extends only slightly beyond the metallic (nonluminescent) WN layer,

a)Electronic mail: shen.234@osu.edu.

Downloaded 25 May 2011 to 128.103.149.52. Redistribution subject to AIP license or copyright; see http://apl.aip.org/about/rights_and_permissions

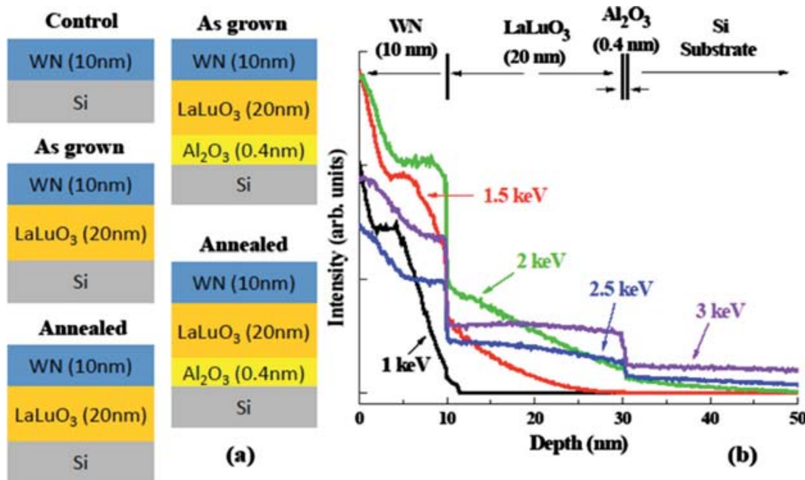

FIG. 1. (Color online) (a) Structures of five samples studied in this work; (b) Monte Carlo simulation of *e-h* rate of pair creation vs depth, normalized to constant power.

$E_B = 1.5$ keV excitation extends past the WN into the $LaLuO_3$ primarily, while higher E_B excite the $LaLuO_3$, Al_2O_3, and Si substrate. Electron-hole pairs generated in Si either recombine in Si or diffuse back to recombine at the $LaLuO_3/Al_2O_3$ interface. Here we focus only on the thin high-*k* layer with E_B from 1 and 1.5 keV.

We used a WN/Si control sample to measure and subtract out the spectral contribution of the WN surface, whose oxidized surface can luminesce. $E_B = 1$ and 1.5 keV WN/Si spectra are subtracted from their respective $WN/LaLuO_3/Si$ and $WN/LaLuO_3/Al_2O_3/Si$ spectra, improving signal-to-noise. Using Monte Carlo simulations[15] to normalize the $E_B = 1$ keV contribution to the $E_B = 1.5$ keV spectra, one obtains differential spectra shown in Fig. 2 corresponding to only the $LaLuO_3$ film and its WN, Si, and Al_2O_3/Si interfaces.

As-grown $WN/LaLuO_3/Si$ exhibits strong peak intensity at 3.8, 4.2, and 4.7 eV, plus weaker peaks at 2.5, 3.1, and 5.5 eV. The 5.5 eV feature corresponds to the near band edge (NBE) transition of $LaLuO_3$. Annealing removes the 5.5, 4.7, and 4.2 eV peaks but introduces a dominant new peak at ~3.8 eV. The as-grown $WN/LaLuO_3/Al_2O_3/Si$ stack also shows strong 4.2 and 4.7 eV peaks. In contrast to the stack without annealing, however, it exhibits no 3.8 and 2.5 eV emissions and much weaker 3.1 eV peak strength. Furthermore, annealing the $WN/LaLuO_3/Al_2O_3/Si$ stack not only suppresses the 3.8 eV peak but also removes the 3.1 eV feature and increases the 5.5 eV peak.

These DRCLS results are consistent with XTEM images of their corresponding structures. Figure 3(a) shows an atomically abrupt interface between the as-deposited $LaLuO_3$ and the Si substrate. After an oxygen anneal, this $LaLuO_3/Si$ junction exhibits a broadened junction with an interfacial layer (IL) of ~0.7 nm. In contrast, the $LaLuO_3/Al_2O_3/Si$ structure with the ultrathin Al_2O_3 IL reveals an abrupt interface between $LaLuO_3$ and Al_2O_3/Si. This interface remains intact after oxygen treatment.

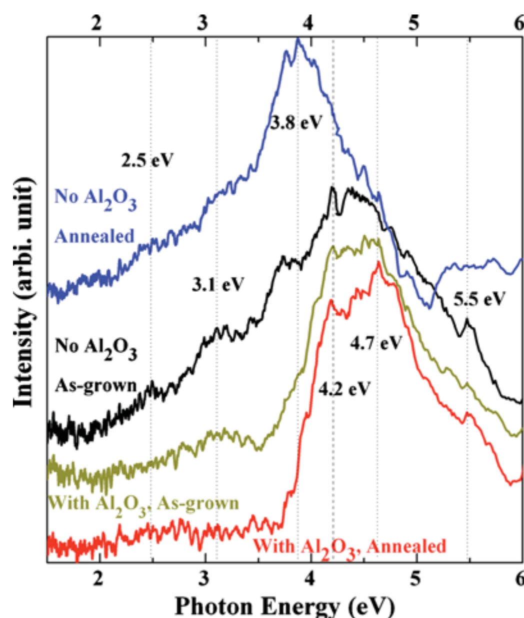

FIG. 2. (Color online) $E_B = 1.5/1.0$ keV differential DRCLS spectra for $WN/LaLuO_3/Si$ and $WN/LaLuO_3/Al_2O_3/Si$ MOS stacks before and after oxygen anneals. An Al_2O_3 IL suppresses growth of the 3.8 eV defect emission otherwise induced by an oxygen anneal.

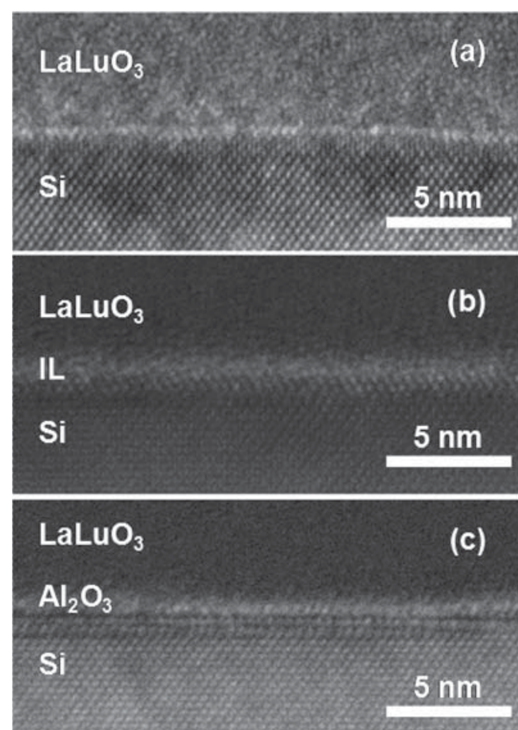

FIG. 3. XTEM images showing: (a) sharp interface at as-deposited $LaLuO_3/Si$ stack interface, (b) an IL of ~0.8 nm at the oxygen-treated $LaLuO_3/Si$ stack, and (c) an abrupt interface at the as-deposited $LaLuO_3/0.4$ nm$-Al_2O_3/Si$ stack that remains intact after oxygen treatment.

Downloaded 25 May 2011 to 128.103.149.52. Redistribution subject to AIP license or copyright; see http://apl.aip.org/about/rights_and_permissions

The features shown in Figs. 2 and 3 illustrate the effect of chemical interactions on the $LaLuO_3/Si$ interface electronic properties. The IL formed between $LaLuO_3$ and Si shown in Fig. 3(b) appears related to the pronounced increase of the 3.8 eV peak and disappearance of the NBE peak in the as-grown $WN/LaLuO_3/Si$ after annealing. With the Al_2O_3 interlayer present, the interface shown in Fig. 3(c) remains abrupt, consistent with the absence of the 3.8 eV peak and the retention of the NBE peak in the annealed $WN/LaLuO_3/Al_2O_3/Si$ spectrum in Fig. 2. An additional benefit of the Al_2O_3 interlayer is that oxygen post-growth annealing removes the 2.5 and 3.1 eV defects without introducing new traps.

Previous work can explain the nature of the major luminescence features in Fig. 2. Here the highest energy feature at 5.5 eV is attributed to the NBE emission of $LaLuO_3$, in agreement with values of 5.3–5.6 eV from internal photoemission.[2] Thus lower energy features must be defect-related. The pair of 4.2 and 4.7 eV peak features evident in all DRCLS spectra are in good agreement with first-principle calculations for the two charge state levels of oxygen vacancies (V_O), the most energetically-favorable native point defects in $LaLuO_3$, at approximately 4.0 and 4.8 eV.[10] The pronounced growth of the 3.8 eV peak is strongly related to interdiffusion and possibly silicate formation, as observed previously from infrared absorption[16] and analogous to electronically-active defects introduced by annealing at HfO_2/Si interfaces.[8] Its small but finite presence in the as-grown $WN/LaLuO_3/Si$ spectrum even before annealing agrees with a very thin lanthanum silicate layer reported for La_2O_3 following ALD on Si,[16] so it is not an intrinsic $LaLuO_3$ defect.

Temperature-dependent I-V measurements of leakage conduction of a similar MOS capacitor with as-deposited $LaLuO_3$ (Ref. 13) indicates a trap level 0.6–0.7 eV below the conduction band based on Pool–Frenkel emission model.[17] Trap 0.7 eV below the conduction band lies 4.8 eV above the valence band, matching closely with the dominant 4.7 eV defect peak in all but the as-grown annealed $WN/LaLuO_3/Al_2O_3/Si$ spectra of Fig. 2. Given the V_O nature of this peak,[10] I-V and DRCLS results indicate that the higher lying oxygen vacancy (V_O^+) facilitates leakage through $LaLuO_3$ films.

Thus DRCLS, TEM, and I-V studies of ultrathin $LaLuO_3$ MOS structures show multiple deep levels in a 5.5 eV band gap, the highest lying pair of which correspond to theoretically predicted neutral and charged oxygen vacancies. Temperature-dependent I-V measurements confirm the dominance of the highest lying of these defects electrically and optically. Overall, an ultrathin Al_2O_3 interlayer permits oxygen annealing of $metal/LaLuO_3/Si$ capacitors to remove native point defects while suppressing $LaLuO_3$ interdiffusion and new trap formation.

Dow Electronic Materials supplied the precursors for lanthanum and lutetium. Some of this work was performed at the Center for Nanoscale Systems (CNS) at Harvard University. Harvard CNS is a member of the National Nanotechnology Infrastructure Network (NNIN).

[1] D. G. Schlom and J. H. Haeni, MRS Bull. **27**, 198 (2002).
[2] J. M. J. Lopes, M. Roeckerath, T. Heeg, E. Rije, J. Schubert, S. Mantl, V. V. Afanas'ev, S. Shamuilia, A. Stesmans, Y. Jia, and D. G. Schlom, Appl. Phys. Lett. **89**, 222902 (2006).
[3] M. Roeckerath, T. Heeg, J. M. J. Lopes, J. Schubert, S. Mantl, A. Besmehn, P. Myllymaki, and L. Niinisto, Thin Solid Films **517**, 201 (2008).
[4] B. H. Lee, J. Oh, H. H. Tseng, R. Jammy, and H. Huff, Mater. Today **9**, 32 (2006).
[5] L. J. Brillson, J. Vac. Sci. Technol. B **19**, 1762 (2001).
[6] S. T. Bradley, S. H. Goss, J. Hwang, W. J. Schaff, and L. J. Brillson, Appl. Phys. Lett. **85**, 1368 (2004).
[7] D. E. Walker, Jr., R. C. Fitch, Jr., J. K. Gillespie, G. H. Jessen, P. D. Cassity, J. R. Breedlove, and L. J. Brillson, Appl. Phys. Lett. **89**, 183523 (2006).
[8] S. Walsh, L. Fang, J. K. Schaeffer, E. Weisbrod, and L. J. Brillson, Appl. Phys. Lett. **90**, 052901 (2007).
[9] J. Schäfer, A. P. Young, L. J. Brillson, H. Niimi, and G. Lucovsky, Appl. Phys. Lett. **73**, 791 (1998).
[10] K. Xiong and J. Robertson, Appl. Phys. Lett. **95**, 022903 (2009).
[11] R. Viturro, M. L. Slade, and L. J. Brillson, Phys. Rev. Lett. **57**, 487 (1986).
[12] J. S. Becker, S. Suh, S. Wang, and R. G. Gordon, Chem. Mater. **15**, 2969 (2003).
[13] Y. Liu, S. Shen, L. Brillson, and R. G. Gordon, Appl. Phys. Lett. **98**, 122908 (2011).
[14] P. Hovington, D. Drouin, and R. Gauvin, Scanning **19**, 1 (1997).
[15] S. Shen, Y. Liu, R. G. Gordon, and L. J. Brillson, "Depth-resolved cathodoluminescence spectrocopy of ultrathin amorphous high-K dielectric $LaLuO_3$," (unpublished).
[16] J. Kwon, M. Dai, M. D. Halls, E. Langereis, Y. J. Chabal, and R. G. Gordon, J. Phys. Chem. C **113**, 654 (2009).
[17] S. M. Sze, *Physics of Semiconductor Devices*, 2nd ed. (Wiley, New York, 1981).

Downloaded 25 May 2011 to 128.103.149.52. Redistribution subject to AIP license or copyright; see http://apl.aip.org/about/rights_and_permissions